Journal of Catalysis 263 (2009) 315–320

Contents lists available at ScienceDirect

Journal of Catalysis

www.elsevier.com/locate/jcat

Alkene hydrogenation on metal surfaces: Why and when are Pd overlayers more efficient catalysts than bulk Pd?

Ana Valcarcel, Franck Morfin, Laurent Piccolo *

Université Lyon 1, CNRS, UMR 5256, IRCELYON, Institut de recherches sur la catalyse et l'environnement de Lyon, 2 avenue Albert Einstein, F-69626 Villeurbanne, France

ARTICLE INFO

Article history:
Received 9 December 2008
Revised 7 February 2009
Accepted 20 February 2009
Available online 17 March 2009

Keywords:
Alkene
Butadiene
Hydrogenation
Absorption
Palladium
Alloy
Single crystal

ABSTRACT

Previous works have shown that palladium overlayers (Pd/Ni, Pd/Cu) are more active than pure Pd surfaces for alkene hydrogenation. These results have been ascribed to the specific nanostructure of the alloy surfaces. Here, we compare Pd(100), Pd(110) and Pd_8Ni_{92}(110) single-crystal surfaces toward 1,3-butadiene hydrogenation and hydrogen absorption, using a gas-phase static reactor. We show that the lower rate of butene formation on clean Pd surfaces can in fact be explained by the initial fast diffusion of hydrogen into the Pd crystal (conversely, hydrogen dissolution in Pd–Ni is negligible). However, the activity of Pd becomes higher at steady state, i.e. after several reaction cycles, due to the increase of the near-surface H concentration. Unlike the butane formation rate, the partial hydrogenation rate appears poorly affected by the Pd surface structure. These results suggest that, when hydrogen supply is rate-determining, hydrogen absorption effects can be more critical than structural effects for Pd-catalyzed hydrogenations.

1. Introduction

Metal nanoparticles are widely used to catalyze chemical reactions. For sizes larger than ~5 nm, less than ~20% of the metal atoms are located at the particle surface, i.e., in many aspects particles behave like extended single-crystal surfaces. Therefore, the latter are valuable models to unravel the mechanisms of surface chemistry [1,2].

Catalytic hydrogenation of hydrocarbons on platinum-group metals is of great importance in refining processes and petrochemistry. The partial hydrogenation of 1,3-butadiene is industrially used to purify C_4 cuts before polymerization or alkylation, but total hydrogenation to butane should be avoided [3]. As butadiene is the simplest conjugated diene, its conversion to butene has been used as a model reaction for selective diene hydrogenation, and more generally for alkene hydrogenation, in various fundamental studies [4–14]. Palladium is the most active and selective metal for this reaction, but its properties can still be improved, e.g., by particle-shape control [14] or alloying [13].

Moss et al. have early reported that Pd–Ni alloy films (with Pd-rich surface) are more active than either pure metal for ethylene hydrogenation [15]. More recently, Bertolini and coworkers have extensively investigated the structural and catalytic properties of Pd–Ni alloy surfaces and of Pd deposits over (essentially inert) Ni substrates [10–12,16]. It has been shown that bimetallic systems are much more active than pure Pd for the selective hydrogenation of butadiene to butenes. Sautet and coworkers have attempted to relate this striking result to the specific nanostructure of Pd/Ni surfaces, which would influence their chemical properties [17]. In particular, the most active alloy surface, Pd_8Ni_{92}(110), exhibits a complex "saw-tooth" reconstruction caused by the relaxation of the strain induced by the larger size of surface-segregated Pd atoms over Ni atoms [10–12,18].

Besides, there is presently a renewed interest in the specific catalytic reactivity of surface metal hydrides, oxides or carbides, with respect to the pure metals [19–24]. Palladium is a very efficient hydrogenation catalyst, but it also acts as a hydrogen sponge [25], for which H absorption follows dissociative H_2 adsorption. Therefore, the interplay between surface reaction and hydrogen dissolution has to be taken into account when looking at catalytic hydrogenation on Pd [13,21–24,26–31]. However, very few works have characterized hydrogen absorption at well-defined Pd-based surfaces under industrially relevant pressure conditions [32–34].

Here, by comparing Pd and Pd_8Ni_{92} single-crystal surfaces toward butadiene hydrogenation, we revisit the question of the superior partial-hydrogenation activity of Pd layers with respect to bulk Pd. Using an original method which allows us to simultaneously measure the hydrogen absorption rate and the hydrogenation rate, we point out the dramatic role of hydrogen dissolution in the reaction kinetics.

* Corresponding author. Fax: +33 472445399.
E-mail address: laurent.piccolo@ircelyon.univ-lyon1.fr (L. Piccolo).
URL: http://laurentcp.googlepages.com/ (L. Piccolo).

0021-9517/$ – see front matter
doi:10.1016/j.jcat.2009.02.023

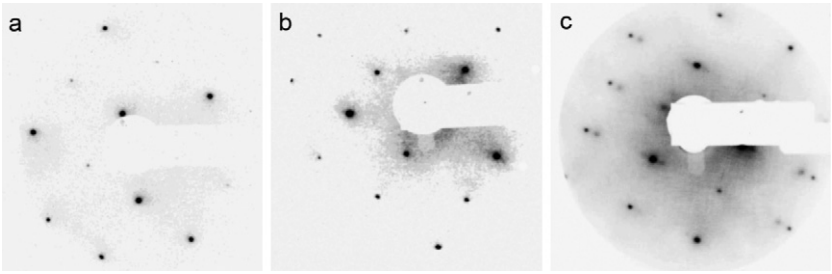

Fig. 1. Low energy electron diffraction patterns of the clean surfaces annealed at ~700 °C under UHV: (a) Pd(100), primary electron energy 156 eV; (b) Pd(110), 122 eV; (c) Pd_8Ni_{92}(110), 144 eV. From the original photographs, the gray levels were inverted and the contrast was increased to improve the pattern readability.

2. Experimental

The experiments were performed with an apparatus coupling an ultrahigh-vacuum (UHV) system for sample preparation and structural characterization with an elevated-pressure low-volume reactor for kinetic analysis of catalytic reactions.

The high-purity Pd(100), Pd(110) and Pd_8Ni_{92}(110) samples were discs of 10.3 ± 0.1 mm diameter and 1 mm thickness. They were grown, oriented (within 0.1°) and polished (roughness <30 nm) by the furnishers. The surfaces were prepared by repeating cycles of Ar^+ sputtering and annealing under UHV (base pressure 10^{-10} Torr) until no impurities could be detected by Auger electron spectroscopy (AES) and sharp diffraction patterns were obtained by low energy electron diffraction (LEED). The clean well-ordered Pd(100), Pd(110) and Pd_8Ni_{92}(110) exhibited (1 × 1), (1 × 1) and (N × 1) surface structures, respectively (Fig. 1). For the latter, the main bright spots corresponding to the (110)–(1 × 1) structure are surrounded by pairs of diffuse satellite spots related to the (N × 1) reconstruction. For $5 < N < 9$, the surface exhibits a roughly constant stability [18]. In the case of Fig. 1c, $N = 6$.

The catalytic tests were performed in a static stainless-steel reaction cell (volume 120 cm^3) communicating with the above-mentioned UHV setup *via* a double-transfer system [13]. The gas mixtures were prepared in a separate chamber (volume ~1 L), which can be evacuated down to 10^{-9} Torr by a dry turbomolecular pumping group. The gas mixer contains various high-purity gas entries and two complimentary capacitance diaphragm gauges (10^{-3}–10^3 Torr). The cell is closed with a gate valve, and evacuated to UHV with the help of a second dry turbomolecular pumping group. It is separated from the gas mixer by an all-metal valve for gas injection and from the quadrupole mass spectrometry (MS) analysis chamber (base pressure 10^{-10} Torr) by a high-precision leak valve.

The reaction kinetics was followed by sampling continuously the reactor's content and recording MS peaks with $m/z = 2$, 40, 54, 56 and 58, which correspond to the masses of H_2, Ar, C_4H_6 (butadiene), C_4H_8 (butenes; the three isomers were not distinguished) and C_4H_{10} (butane) molecules, respectively. After normalization by the Ar signal, the data were corrected for ion fragmentation and spectrometer sensitivity to obtain partial pressures (Appendix A.1).

It should be noted that: (i) the oil diffusion pump (capped with a liquid nitrogen trap) which was used in the MS analysis chamber, allowed excellent evacuation of all the gases, without any accumulation; (ii) blank tests (without sample) were performed to check the reactor for inertness; (iii) the H_2 pressure was kept sufficiently low to avoid the formation of the β-hydride phase in the bulk of Pd single crystals [25].

3. Results and discussion

Fig. 2 plots butadiene-to-butene hydrogenation turnover frequency (TOF) versus molecular hydrogen pressure (p_{H_2}) for initial and stationary runs on Pd and Pd–Ni (110) surfaces. The TOF is the number of hydrocarbon molecules converted per surface atom per unit of time, here measured at the beginning of each conversion process. *Initial run* and *stationary run* denote the reaction on the freshly prepared surface and the reaction performed after several cycles leading to stationary kinetics, respectively. Each cycle consisted of a reaction run followed by gas evacuation for 5 min. The number of cycles required to reach this dynamic equilibrium was between 2 and 4, depending on the reaction conditions.

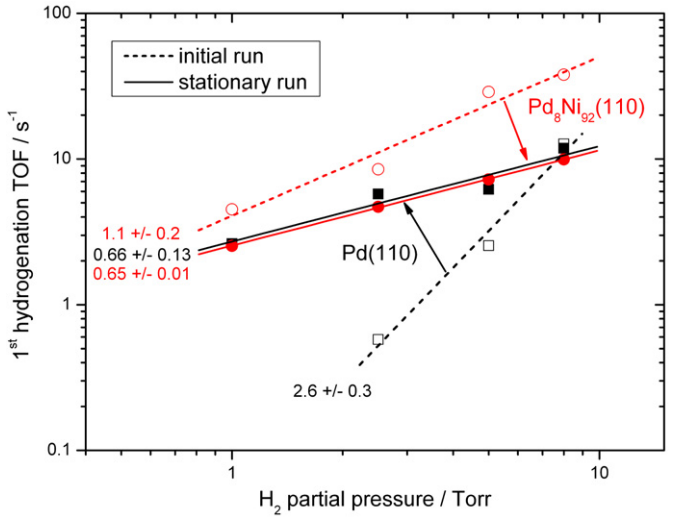

Fig. 2. Turnover frequency of butadiene hydrogenation to butene versus initial H_2 pressure over Pd(110) (squares) and Pd_8Ni_{92}(110) (circles) during runs on the fresh surfaces (open symbols and dashed lines) and stationary runs (filled symbols and straight lines). The slopes of the linear fits, yielding the reaction orders toward H_2, are indicated. Conditions: 25 °C, initial butadiene pressure 0.5 Torr (1 Torr = 133 Pa).

It is observed that fresh Pd–Ni is more active than fresh Pd, especially at low H_2 pressures. However, Pd–Ni partly deactivates and Pd activates throughout the reaction cycles, in such a way that the catalysts reach quite a similar activity at steady state. For example, at 25 °C, for initial hydrogen and butadiene pressures of 5 and 0.5 Torr, respectively, fresh Pd–Ni is 11 times more active than fresh Pd for butene formation. Both turnover frequencies stabilize at 6–7 s^{-1} after several cycles (Fig. 2).

It is known that the partial-hydrogenation rate is almost independent of the butadiene pressure ($p_{C_4H_6}$),[1] since the butadiene coverage is always high [3]. Here, since a power rate-law is obeyed in each case ($TOF \propto p_{H_2}^x$), reaction partial orders x toward H_2 have been determined. It appears that the partial order is much higher for fresh Pd (2.6) than for fresh Pd–Ni (1.1) and for reacted Pd and Pd–Ni (0.7). Thus, on clean Pd(110), the reaction is clearly limited by the lack of hydrogen.

[1] For example, for Pd–Ni at 25 °C with $p_{H_2} = 8$ Torr, $TOF \propto p_{C_4H_6}^y$ with $y = -0.25 \pm 0.11$.

The transient behavior of butene formation and consumption over Pd(110) in a particular set of conditions is analyzed in Figs. 3a and 3b. As expected for Pd-based catalysts, butane is formed after quasi-complete conversion of butadiene to butene, i.e., the selectivity to butene (butene formation rate divided by butadiene consumption rate) is higher than 90%. Fig. 3c shows the H_2 pressure (top curves) and the atomic hydrogen uptake (bottom curves) during the same experiment. The latter was derived from the loss of H in the gas phase, which was calculated from all the partial pressures by taking into account the conservation of atomic hydrogen (Appendix A.2). It appears that during the first run, a significant amount of hydrogen diffuses into the bulk of Pd(110), i.e., H uptake increases with time. More specifically, it is seen (Fig. 3c) that H absorption continuously slows down in the course of the first hydrogenation step (the rate of which simultaneously increases, see Fig. 3a). As soon as the second hydrogenation step begins, H absorption accelerates, due to the decreased hydrocarbon coverage present during the second hydrogenation step [13]. It should be noted that, since the H uptake is high and the hydrogen desorption from the Pd crystal is moderate at room temperature, the initial hydrogen concentration for run $N+1$ is similar to the final one in run N. In stationary runs on Pd(110), hydrogen dissolution becomes negligible during the first hydrogenation step (H uptake is zero, Fig. 3c), in correlation with faster hydrogenation (Fig. 3b). Then, as for initial runs, H absorption markedly accelerates when the second step begins, and finally slows down and adopts a roughly constant rate at long reaction times.

Repeated experiments under various conditions confirm that the larger the amount of hydrogen absorbed throughout a reaction run, the more Pd(110) is active in the subsequent run, until saturation. In the experiment depicted in Fig. 4, the first run was stopped early (before the onset of the second hydrogenation) on purpose. This way, a moderate amount of H was absorbed during run 1 (Fig. 4b), which led to a moderate increase of the first hydrogenation rate in run 2 (Fig. 4a). Similarly, as the duration of run 2 was chosen longer, more H was absorbed during this run, which led to an increased reaction rate in run 3, etc.

An additional experiment with sequential pre-exposure to pure H_2, evacuation of the residual gas and butadiene hydrogenation reaction has allowed us to check that pre-saturation of the subsurface with hydrogen indeed correlates with a maximum hydrogenation activity (Fig. 5). As a matter of fact, by comparing the slope of $P_{C_4H_6}(t)$ with that in Fig. 3b, it is observed that after the pre-absorption run, the maximum (stationary) rate of butadiene hydrogenation is directly reached. The atomic hydrogen uptake in Pd(110) at the end of the pre-absorption run is 30% of the amount initially introduced (to be compared to 15%, Fig. 3c), while no H is absorbed during the reaction run itself (not shown).

Although non-zero, hydrogen dissolution in $Pd_8Ni_{92}(110)$ was quite low. Using our global method, the hydrogen uptake could not be measured with reasonable accuracy. Actually, low absorption was expected since the bulk of the crystal is Ni-rich, and crystalline Ni absorbs much less hydrogen than Pd under our mild conditions [35].[2] Moreover, surface segregation of Pd leads only to 1 atom-thick pure Pd overlayer [10–12]. The partial deactivation of the catalyst observed in Fig. 2 is ascribed to carbon deposition following possible hydrocarbon cracking on the surface. Indeed, a significant amount of carbon was detected on the Pd–Ni surface by Auger electron spectroscopy after the reactions, while the Pd surfaces remained essentially clean. In the case of Fig. 6, the Pd + C peak (~277 eV)/Pd peak (330 eV) intensity ratio, used to estimate the C amount, increased from 22% (clean surface) to 37% (up to 44% in some experiments). On the other hand, the same ratio in-

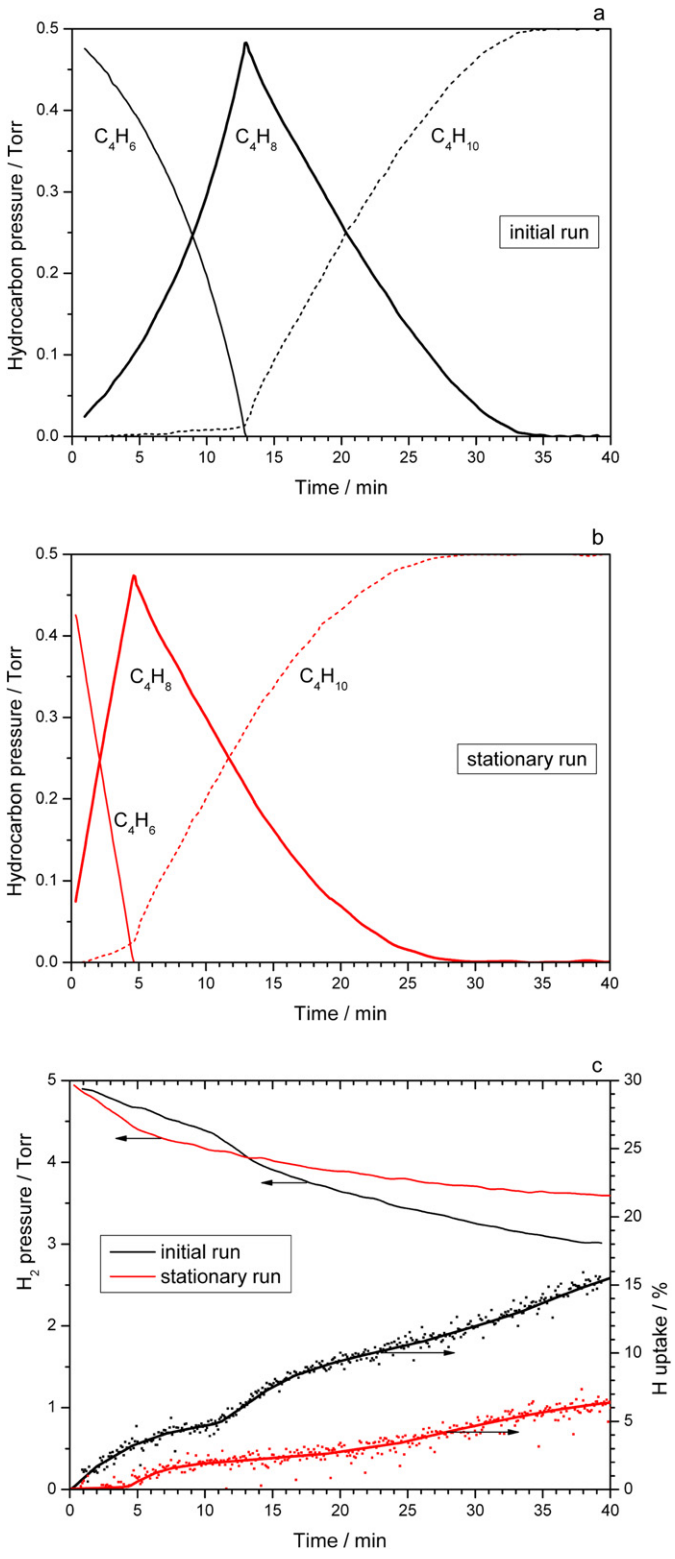

Fig. 3. (a) Partial pressures of hydrocarbons during hydrogenation of butadiene over Pd(110) during the *first* run. (b) Same as (a) for a *stationary* run. (c) Partial pressure of H_2 (thin lines, left scale) and H uptake (dots and thick lines, right scale) throughout the same reaction runs as in (a) and (b). The H uptake is expressed as an atomic percentage of the number of H atoms introduced in the reactor at $t = 0$. Raw H uptake data are plotted together with polynomial fits improving readability. Conditions: same as in Fig. 2 and initial H_2 pressure 5 Torr.

[2] By modeling the $Pd_8Ni_{92}(110)$ surface by a Pd monolayer over a Ni(110) substrate (Ref. [18]), we have found by density-functional theory calculations that the H atoms can only be absorbed under the shifted Pd atoms of the surface reconstruction (A. Valcarcel, D. Loffreda, F. Delbecq, L. Piccolo, unpublished results).

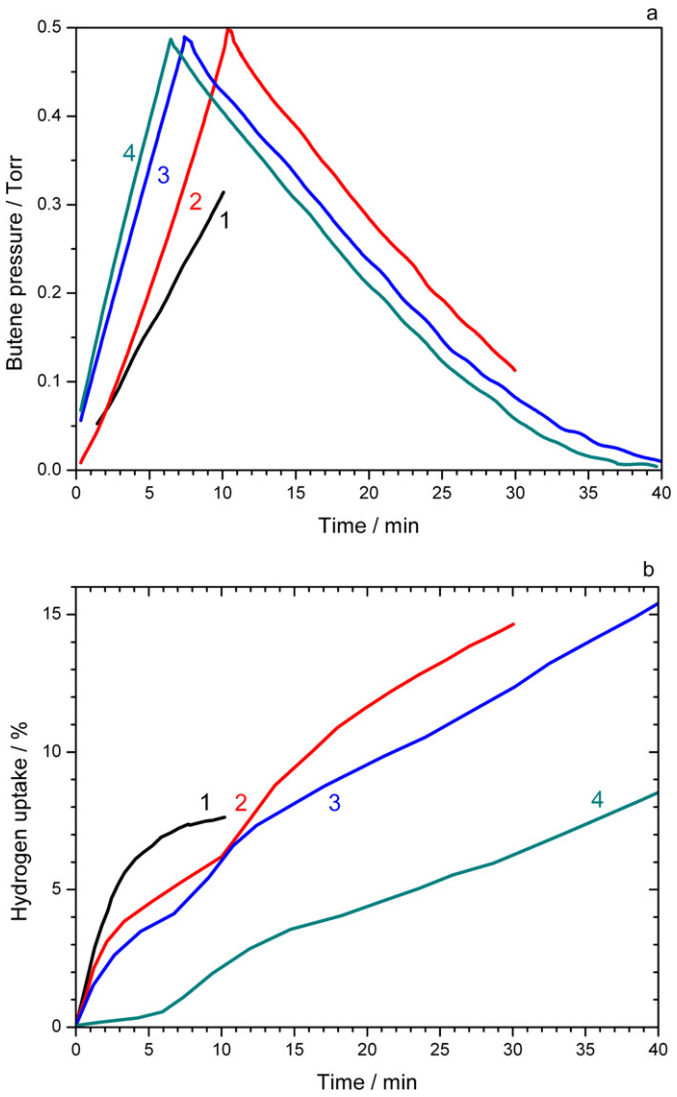

Fig. 4. Evolution of the butene pressure (a) and hydrogen uptake (b) during 4 successive cycles of butadiene hydrogenation over Pd(110). Conditions: same as in Fig. 3.

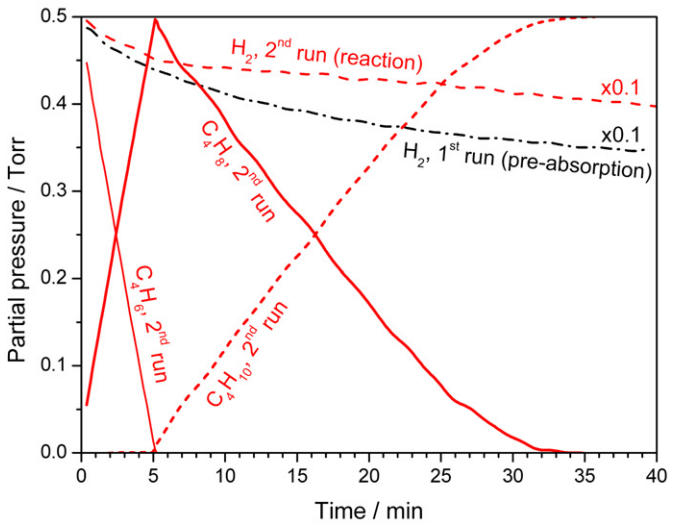

Fig. 5. Partial pressure of hydrogen and hydrocarbons versus time. In the first run, clean Pd(110) was exposed to pure H_2 (5 Torr) at 25 °C. Then residual H_2 was evacuated and the sample was exposed (second run) to a mixture of butadiene (0.5 Torr) and H_2 (5 Torr).

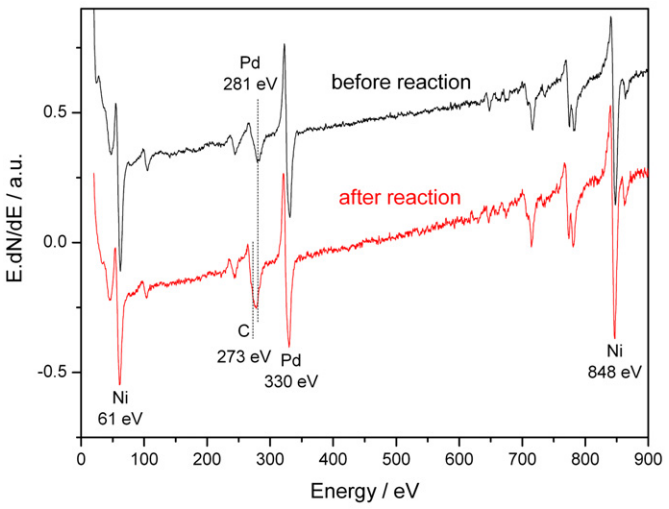

Fig. 6. Auger electron spectra recorded before (top) and after (bottom) butadiene hydrogenation (25 °C; initial pressures: 1 Torr H_2, 0.5 Torr C_4H_6; 3 reaction runs of 1 h each) on $Pd_8Ni_{92}(110)$.

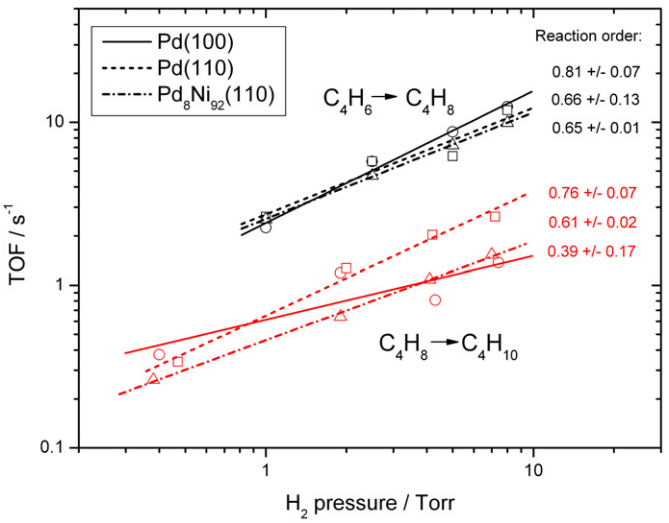

Fig. 7. Stationary turnover frequencies versus H_2 pressure for butadiene hydrogenation to butene (top) and butene hydrogenation to butane (bottom), on Pd(100) (straight lines), Pd(110) (dashed lines) and $Pd_8Ni_{92}(110)$ (dash-dotted lines). The slopes of the linear fits, indicated at the right, provide the reaction orders toward H_2. Conditions: same as in Fig. 2.

creased from 19% for clean Pd surfaces to only 20–21% for the reacted ones.

In addition, no significant restructuring occurs when $Pd_8Ni_{92}(110)$ is exposed to butadiene–hydrogen mixtures, as demonstrated by in-situ surface X-ray diffraction [12]. Hence, taking into account the fraction of Pd sites poisoned by C on Pd–Ni, the active sites of the Pd layer appear *intrinsically more active* than those of the bulk Pd surface since the overall steady-state activities are similar (Fig. 2). This close similarity is then due to a combination of effects (dissolution in Pd and partial poisoning of Pd–Ni) and has no physical meaning.

To assess the influence of surface structure on hydrogenation kinetics, we have also investigated the reactivity of Pd(100), following protocols identical to those employed for (110) samples. To our knowledge, Pd(100) has never been investigated in butadiene hydrogenation under elevated pressure. Fig. 7 shows that the stationary reaction kinetics is similar to that of Pd(110) and $Pd_8Ni_{92}(110)$. The turnover frequencies associated to the first hy-

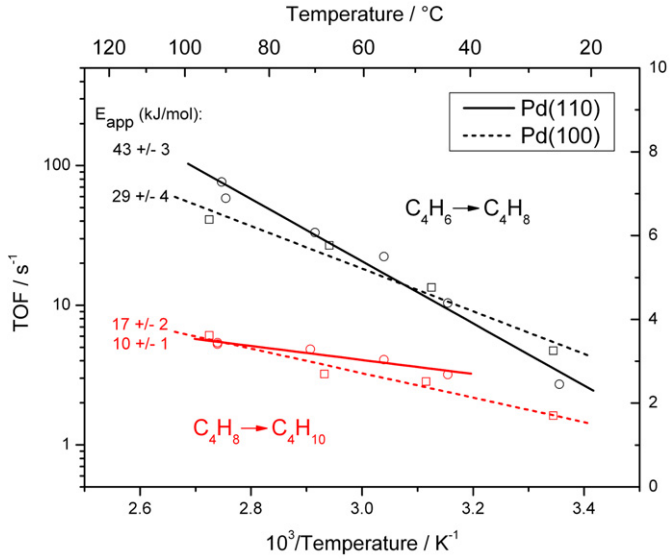

Fig. 8. Arrhenius plot of stationary turnover frequencies for butadiene hydrogenation to butene (TOF_1, top) and butene hydrogenation to butane (TOF_2, bottom), for Pd(110) (circles and straight lines) and Pd(100) (squares and dashed lines). The slopes of the linear fits (apparent activation energy E_{app} in kJ/mol) are indicated. Initial pressures: 4 Torr C_4H_6, 8 Torr H_2. Notice that the TOF_1/TOF_2 ratio increases with temperature, i.e., Pd is more selective at higher temperatures.

drogenation step are nearly identical for all three systems. Only for butane formation, Pd–Ni is slightly less active than Pd.[3] However, the critical step for total hydrogenation is not the supply of hydrogen but the adsorption of butene [13]. Fig. 8 further shows that, in spite of the different apparent activation energies, the turnover rates are quite similar for (110) and (100) Pd surfaces in the temperature range considered here.

Besides, it should be noted that Ni is not the sole metal promoting Pd in butadiene conversion. The Pd/Cu(110) system, whose structure is different from that of Pd/Ni(110), also exhibits high activity [36,37]. This supports our conclusion: the ability of the bimetallic system to concentrate hydrogen in the vicinity of the surface, i.e., within the Pd layer, is at least as important as its specific structure in terms of alkene hydrogenation.

There have been several attempts to synthesize Ni–Pd core–shell supported nanoparticles in order to mimic the model Pd/Ni surfaces [38,39]. Those have not demonstrated any superiority over Pd catalysts. The present work explains this result by showing that the steady-state activities of Pd and Pd–Ni surfaces are similar provided the Pd bulk is filled with hydrogen.

The superior hydrogenation activity of Pd-rich layers over hydrogen-free Pd single-crystal surfaces can be nicely linked to the work of Freund and coworkers [23,28–30], who have compared Pd nanoparticles with Pd single crystals. They have explained the much higher alkene hydrogenation rate on the particles by their nanoscale dimensions, which allow facile accessibility of active subsurface hydrogen to the alkene molecules [28,29] or a possible enhanced reactivity of hydrogen due to its confinement [30]. The presence of H absorbed in the Pd particle volume would even be *required* for olefin hydrogenation [23]. It should be noted that these works have been performed under UHV conditions, where the supply of reactive hydrogen may be highly rate-limiting. Whether subsurface hydrogen atoms directly interact with hydrocarbon molecules, as previously demonstrated for nickel [40], or if they first undergo an adsorbed state is still not clear. Anyhow, in the present case, the loss of (hydrogen) reactant through absorption appears *sufficient* to explain the differences between bulk Pd and Pd overlayers. The gradual saturation of the Pd crystal subsurface by hydrogen provokes a decrease of the dissolution rate, leading to an increased near-surface concentration of H available for the partial hydrogenation of butadiene. As a result, the surface Pd hydride is more active than pure Pd.

In conclusion, for the catalytic system considered here, Ni essentially acts as a support for Pd and prevents the diffusion of hydrogen into the bulk. Conversely, H dissolution in *clean* Pd crystals strongly competes with the surface reactions. However, as the Pd subsurface is being enriched with hydrogen, the catalytic activity of the surface gradually increases.

Similarly to nanoparticles, surface "nanolayers" (here obtained by segregation of palladium at an alloy surface) can exhibit increased catalytic activity with respect to bulk materials by maintaining hydrogen atoms in the near-surface region. This should be considered as a phenomenon of equal importance as electronic effects in catalytic hydrogenation on metal alloys.

Acknowledgments

L.P. thanks Dr. Vincent Robert and Nadège Teyssèdre for valuable comments on the manuscript.

Appendix A

A.1. Calculation of partial pressures from mass spectrometry signals

$$P_{H_2} = P_{Ar}\frac{S_{Ar}}{S_{H_2}}\frac{I_2}{I_{40}},$$

$$P_{C_4H_6} = P_{Ar}\frac{S_{Ar}}{S_{C_4H_6}}\left(\frac{I_{54}}{I_{40}} - F^{54}_{C_4H_8}\frac{I_{56}}{I_{40}} - F^{54}_{C_4H_{10}}\frac{I_{58}}{I_{40}}\right),$$

$$P_{C_4H_8} = P_{Ar}\frac{S_{Ar}}{S_{C_4H_8}}\left(\frac{I_{56}}{I_{40}} - F^{56}_{C_4H_{10}}\frac{I_{58}}{I_{40}}\right),$$

$$P_{C_4H_{10}} = P_{Ar}\frac{S_{Ar}}{S_{C_4H_{10}}}\frac{I_{58}}{I_{40}}.$$

P_I: Partial pressure of product I,

S_I: Sensitivity of the spectrometer to product I.

Sensitivity factors can be adjusted thanks to carbon mass conservation (sorption neglected):

$$P_{C_4H_6} + P_{C_4H_8} + P_{C_4H_{10}} = P_{C_4H_6}(t=0).$$

I_i: Intensity of the spectrometer peak at $m/z = i$,

F^i_J: Fragmentation of product J into ion of $m/z = i$,

$F^{54}_{C_4H_8} = 6.0\%$; $F^{54}_{C_4H_{10}} = 2.0\%$; $F^{56}_{C_4H_{10}} = 6.5\%$.

Argon ($m/z = 40$) is used for internal calibration.

A.2. Calculation of hydrogen uptake from partial pressures

$$n^{abs}_H = 100\frac{N^{gas}_H(t=0) - N^{gas}_H}{N^{gas}_H(t=0)} \quad \text{(loss of gas-phase H)}$$

with:

$$N^{gas}_H = (2P_{H_2} + 6P_{C_4H_6} + 8P_{C_4H_8} + 10P_{C_4H_{10}})\frac{V}{kT} \quad \text{(perfect-gas law)}$$

with:

$$P_{C_4H_8} = P_{C_4H_8}(t=0) - P_{C_4H_6} - P_{C_4H_{10}}.$$

[3] The difference increases at higher conversions (not shown). Note that this selectivity aspect, although interesting both from fundamental and practical points of view, has never been reported to our knowledge.

n_H^{abs}: Hydrogen uptake, i.e., percentage of hydrogen atoms diluted in the crystal with respect to the amount introduced at $t = 0$ (adsorption neglected),

N_H^{gas}: Number of hydrogen atoms in the gas phase,

V: Volume of the reactor ($V = 120$ cm^3),

k: Boltzmann's constant,

T: Temperature of the reactor.

References

[1] G.A. Somorjai, Introduction to Surface Chemistry and Catalysis, Wiley, New York, 1994.
[2] G. Ertl, Angew. Chem. Int. Ed. 47 (2008) 3524.
[3] J.P. Boitiaux, J. Cosyns, S. Vaudevan, Appl. Catal. 6 (1983) 41.
[4] C.M. Pradier, E. Margot, Y. Berthier, J. Oudar, Appl. Catal. 43 (1988) 177.
[5] X.C. Guo, R.J. Madix, J. Catal. 155 (1995) 336.
[6] C. Yoon, M.X. Yang, G.A. Somorjai, Catal. Lett. 46 (1997) 37.
[7] S. Katano, H.S. Kato, M. Kawai, K. Domen, J. Phys. Chem. B 107 (2003) 16.
[8] J. Sylvestre-Albero, G. Rupprechter, H.J. Freund, J. Catal. 235 (2005) 52.
[9] C. Breinlich, J. Haubrich, C. Becker, A. Valcarcel, F. Delbecq, K. Wandelt, J. Catal. 251 (2007) 123.
[10] J.C. Bertolini, Appl. Catal. A 191 (2000) 15, and references therein.
[11] M. Abel, Y. Robach, J.C. Bertolini, L. Porte, Surf. Sci. 454–456 (2000) 1.
[12] M.C. Saint-Lager, Y. Jugnet, P. Dolle, L. Piccolo, R. Baudoing-Savois, J.C. Bertolini, A. Bailly, O. Robach, C. Walker, S. Ferrer, Surf. Sci. 587 (2005) 229.
[13] L. Piccolo, A. Piednoir, J.C. Bertolini, Surf. Sci. 592 (2005) 169.
[14] L. Piccolo, A. Valcarcel, M. Bausach, C. Thomazeau, D. Uzio, G. Berhault, Phys. Chem. Chem. Phys. 10 (2008) 5504.
[15] R.L. Moss, D. Pope, H.R. Gibbens, J. Catal. 46 (1977) 204.
[16] J.S. Filhol, M.C. Saint-Lager, M. De Santis, P. Dolle, D. Simon, R. Baudoing-Savois, J.C. Bertolini, P. Sautet, Phys. Rev. Lett. 89 (2002) 146106.
[17] J.S. Filhol, D. Simon, P. Sautet, J. Am. Chem. Soc. 126 (2004) 3228.
[18] A. Valcarcel, D. Loffreda, F. Delbecq, L. Piccolo, Phys. Rev. B 76 (2007) 125406.
[19] D.W. Goodman, C.H.F. Peden, M.S. Chen, Surf. Sci. 601 (2007) L124.
[20] H. Over, M. Muhler, A.P. Seitsonen, Surf. Sci. 601 (2007) 5659.
[21] D. Teschner, J. Borsodi, A. Wootsch, Z. Révay, M. Hävecker, A. Knop-Gericke, S.D. Jackson, R. Schlögl, Science 320 (2008) 86.
[22] D. Teschner, Z. Révay, J. Borsodi, M. Hävecker, A. Knop-Gericke, R. Schlögl, D. Milroy, S.D. Jackson, D. Torres, P. Sautet, Angew. Chem. Int. Ed. 47 (2008) 9274.
[23] M. Wilde, K. Fukutani, W. Ludwig, B. Brandt, J.H. Fischer, S. Schauermann, H.J. Freund, Angew. Chem. Int. Ed. 47 (2008) 9289.
[24] F. Studt, F. Abild-Pedersen, T. Bligaard, R.Z. Sorensen, C.H. Chistensen, J.K. Norskov, Angew. Chem. Int. Ed. 47 (2008) 9299.
[25] E. Wicke, H. Brodowsky, H. Züchner, Appl. Phys. 29 (1978) 73.
[26] W. Palczewska, in: Z. Paal, P.G. Menon (Eds.), Hydrogen Effects in Catalysis, Marcel Dekker, New York, 1988, pp. 378–386.
[27] G. Rupprechter, G.A. Somorjai, Catal. Lett. 48 (1997) 17.
[28] A.M. Doyle, S.K. Shaikhutdnikov, S.D. Jackson, H.J. Freund, Angew. Chem. Int. Ed. 42 (2003) 5240.
[29] A.M. Doyle, S.K. Shaikhutdnikov, H.J. Freund, J. Catal. 223 (2004) 444.
[30] M. Morkel, G. Rupprechter, H.J. Freund, Surf. Sci. 588 (2005) L209.
[31] N.A. Khan, Shaikhutdinov, H.J. Freund, Catal. Lett. 108 (2006) 159.
[32] B.D. Kay, C.H.F. Peden, D.W. Goodman, Phys. Rev. B 34 (1986) 817.
[33] C.H.F. Peden, B.D. Kay, D.W. Goodman, Surf. Sci. 175 (1986) 215.
[34] L. Piccolo, A. Piednoir, J.C. Bertolini, Surf. Sci. 600 (2006) 4211.
[35] B. Baranowski, S.M. Filipek, J. Alloys Compd. 404–406 (2005) 2, and references therein.
[36] L. Constant, P. Ruiz, M. Abel, Y. Robach, L. Porte, J.C. Bertolini, Top. Catal. 14 (2001) 125.
[37] M. Abel, Y. Robach, L. Porte, Surf. Sci. 498 (2002) 244.
[38] A. Renouprez, J.F. Faudon, J. Massardier, J.L. Rousset, P. Delichère, G. Bergeret, J. Catal. 170 (1997) 181.
[39] R. Massard, D. Uzio, C. Thomazeau, C. Pichon, J.L. Rousset, J.C. Bertolini, J. Catal. 245 (2007) 133.
[40] S.T. Ceyer, Acc. Chem. Res. 34 (2001) 737.